Published in final edited form as:
Acta Biomater. 2009 March ; 5(3): 903–912. doi:10.1016/j.actbio.2008.10.003.

Self-assembling peptide–lipoplexes for substrate-mediated gene delivery

Jennifer C. Rea[a], **Romie F. Gibly**[b], **Annelise E. Barron**[c], and **Lonnie D. Shea**[a,d,*]

[a]Department of Chemical and Biological Engineering, Northwestern University, 2145 Sheridan Road, Tech E156, Evanston, IL 60208-3120, USA

[b]Department of Interdepartmental Biological Sciences, Northwestern University, 2145 Sheridan Road, Tech E156, Evanston, IL 60208-3120, USA

[c]Department of Bioengineering, Stanford University, W300B James H. Clark Center, 318 Campus Drive, Stanford, CA 94305-5440, USA

[d]Robert H. Lurie Comprehensive Cancer Center, Northwestern University, Chicago, IL 60611, USA

Abstract

The efficiency of biomaterial-based gene delivery is determined by the interaction of the material and the vector. For lipoplexes, surface immobilization has been used to transfect cells for applications such as cell arrays and model tissue formation through patterned transfection. Further increases in the delivery efficiency are limited by cellular internalization, which may be overcome by altering the material/vector interactions. In this report, we investigated the modification of the lipoplex physical properties through self-assembly with cationic peptides, and subsequently quantified cellular association, internalization and nuclear accumulation of DNA and transfection. Relative to lipid alone, peptide–lipoplexes enhanced transfection by up to 4.6-fold. The presence of the peptide in the lipoplex increased internalization efficiency by up to 4.5-fold, decreased the percentage of lysosomal DNA by 2.1-fold and increased the efficiency of nuclear accumulation by 3.0-fold. In addition, an analysis of internalization pathways for peptide–lipoplexes indicated a greater role of clathrin and caveolae-mediated endocytosis relative to macropinocytois, which was not observed for peptide-free lipoplexes. These results demonstrate peptide-induced enhancement of gene transfer by surface immobilization due to increased cellular internalization and nuclear accumulation, which has numerous applications ranging from cell-based assays to regenerative medicine.

Keywords

Gene delivery; Peptide; Lipoplex; Substrate-mediated; Self-assembly

1. Introduction

Biomaterials have been used for many therapeutic and research applications such as tissue engineering and gene delivery. Gene transfer from the surface of a biomaterial, termed reverse

*Corresponding author. Tel.: +1 847 491 7043; fax: +1 847 491 3728. *E-mail address:* l-shea@northwestern.edu (D. Shea).
Part of the Self-Assembling Biomaterials Special Issue, edited by William L. Murphy and Joel H. Collier.

transfection [1], solid-phase delivery [2] or substrate-mediated delivery [3], immobilizes DNA vectors onto a surface as opposed to more typical bolus delivery from the media. Several approaches have been employed for DNA immobilization, including DNA entrapment in gelatin [1], polyelectrolyte layering of DNA [4,5] and immobilization of preformed complexes followed by specific tethering [3,6,7] or nonspecific adsorption [2,8-12]. Immobilization by non-specific adsorption can reduce the amount of DNA required for expression and increase transgene expression and the number of cells expressing the transgene relative to similar quantities delivered as a bolus [8,9]. However, the delivery efficiency is a function of not only the properties of the surface but also the properties of the DNA complexation vectors, such as cationic polymers or lipids [3,8,10].

Although immobilizing complexes places the vector directly in the cell microenvironment, the immobilization must still allow for efficient cell internalization and intracellular trafficking of the DNA. While transfection following surface immobilization with cationic polymers is limited by intracellular transport, transfection with lipoplexes delivered from the surface is limited by internalization [13]. Increased cellular association of lipoplexes has been achieved for bolus delivery by altering lipoplex physical properties, such as size and zeta potential, and adding functional groups to the lipoplex surface to mediate cellular interactions [14]. However, while DNA complexes formed with cationic polymers, termed polyplexes, have been modified for surface delivery, lipoplexes are more difficult to alter due to the chemical structure of the lipids, such as the lack of covalent binding sites [3].

The physiochemical properties of lipoplexes that influence gene transfer can be manipulated through peptide addition during complex formation [15,16]. We have previously reported that transfection efficiency of lipoplexes delivered as a bolus is significantly enhanced by the addition of short, cationic peptides to form self-assembled particles, termed peptide–lipoplexes [14]. Specifically, these peptides contained the SV40 T-antigen nuclear localization sequence (NLS) or a scrambled NLS sequence, and have amines that facilitate binding between the peptide and plasmid. Peptide–lipoplexes are assembled by first incubating cationic peptides with DNA prior to incubation with lipids. The peptides interact with the DNA without fully shielding its negative charges, as shown by gel electrophoresis, thus allowing the cationic lipids to condense the DNA [14]. Peptide–lipoplexes with a size of less than 500 nm, a positive zeta potential and a relatively largehigh amount of surface-displayed amines had the highest transfection efficiency and highest amount of cell-associated DNA, regardless of peptide sequence [14]. These results suggest that increasing the peptide quantity added to DNA increases the incorporation of peptides into the lipoplexes, which can facilitate cellular interactions through modified lipoplex surface properties [17].

In this report, we investigate the incorporation of peptides as a means of overcoming the limiting steps to substrate-mediated lipofection. We hypothesize that the physical properties of the lipoplexes, which are determined by the amount of peptide added, affect the lipoplex interaction with the substrate, thus affecting cell association, internalization, nuclear accumulation and transfection efficiency. Peptide–lipoplexes were formed at peptide/DNA weight ratios ranging from 0 to 100 by adding cationic peptides to DNA prior to complexation with lipids. Protein expression was quantified as a function of peptide incorporation in the lipoplexes. Lipoplexes were visualized on the surface using fluorescence microscopy to determine lipoplex morphology. Cell association of DNA, DNA internalization efficiency and nuclear accumulation efficiency were measured as a function of peptide amount. Finally, the pathway for internalization and the subsequent lysosomal distribution of DNA were investigated by using endocytic inhibitors and confocal microscopy, respectively. These studies identify mechanisms by which lipoplex delivery from biomaterials can be enhanced and may contribute to the design of gene delivery vectors for use in a range of cell-based assays or regenerative medicine.

2. Materials and methods

2.1. Materials

Plasmids encoding for β-galactosidase (pβGal) and luciferase/enhanced green fluorescent fusion protein (pEGFP-Luc) with a CMV promoter were purified from bacteria culture using Qiagen (Valencia, CA) reagents and stored in Tris–EDTA buffer (10 mM Tris, 1 mM EDTA, pH 7.4). Lipofectamine, SYTO 61 nucleic acid stain and LysoTracker Yellow HCK-123 reagent were purchased from Invitrogen (Carlsbad, CA). Label IT Cy3 Labeling Kit was purchased for Mirus Bio Corporation (Madison, WI). [α-^{32}P]dATP was purchased from PerkinElmer (Waltham, MA). Amino acids and resin for peptide synthesis were purchased from Novabiochem (San Diego, CA). The remaining peptide synthesis reagents were purchased from Applied Biosystems (Foster City, CA). Peptides were also purchased from Celtek Bioscience LLC (Nashville, TN). Amiloride hydrochloride, filipin and chlorpromazine hydrochloride were purchased from Sigma-Aldrich (St. Louis, MO). All other reagents were obtained from Fisher Scientific (Waltham, MA) unless otherwise noted.

2.2 Peptide synthesis and purification

An Applied Biosystems (Foster City, CA) 433A peptide synthesizer was used to synthesize the SV40 T-antigen nuclear localization sequence (NLS) and a scrambled peptide control. The SV40 peptide, EGPKKKRKVG, containing the minimal SV40 T-antigen NLS, and the sSV40 peptide, EKRGKVKPKG, a scrambled version of SV40, were synthesized using standard solid phase methods and FastMocTM chemistry. The peptides were cleaved with a mixture of 90% trifluoroacetic acid, 2.5% triisopropylsilane (TIS), 2.5% thioanosole and 5% water for 1-2 h at room temperature, then lyophilized. The crude peptides were analyzed for purity by reversed-phase high-pressure liquid chromatography (RP-HPLC). The peptides were purified by preparative RP-HPLC with a gradient of 0–20% acetonitrile with 0.1% trifluoroacetic acid (TFA) in water with 0.1% TFA. Peptide molecular weights were confirmed using electrospray ionization (ESI) mass spectroscopy and matrix-assisted laser desorption ionization time-of-flight (MALDI-TOF) mass spectrometry at Northwestern University's Analytical Services Laboratory. Peptide purities were analyzed using analytical RP-HPLC and were determined to be >95%.

2.3. Peptide–lipoplex formation and immobilization

Lipofectamine (Invitrogen, Carlsbad, CA), a 3:1 w/w formulation of the polycationic lipid 2,3-dioleyloxy-*N*-[2(sperminecarboxamido)ethyl]-*N*,*N*-dimethyl-1-propanaminium trifluoroacetate (DOSPA) and the neutral lipid dioleoyl phosphatidylethanolamine (DOPE), was used at a 10:1 w/w ratio with DNA, within the manufacturer's recommended usage range. Peptide–lipoplexes were formed by adding 22.5 μl of peptide solution containing varying amounts of peptide to 22.5 μl DNA solution, and the resulting solution was then mixed by gentle pipetting. The peptide/DNA mixture was allowed to incubate for 20 min at room temperature prior to the dropwise addition of 45 μl of lipid solution. The resulting solution was mixed by gentle pipetting and incubated for 20 min. Peptide–lipoplexes were formed in serum-free cell growth media (Dulbecco's modified Eagle's medium (DMEM), Invitrogen, Carlsbad, CA) at pH 7.4. All peptide/DNA ratios reported herein are by weight; the conversion between peptide/DNA w/w ratio and peptide/DNA N/P ratio is 1 w/w ratio to 1.46 N/P ratio.

Immediately after complex formation, peptide–lipoplexes were immobilized onto a 48-well tissue culture polystyrene plate by adding 30 μl of peptide–lipoplexes to 70 μl of DMEM in each well. Lipoplex formulation and immobilization were modified for other plate formats (e.g. 96-well plate) based on relative surface area. Peptide–lipoplexes were allowed to incubate in the wells at room temperature for 2 h prior to two wash steps with DMEM to remove unbound complexes.

2.4. Cell culture and transfection

Transfection studies were performed with NIH/3T3 and HEK293T cells (ATCC, Manassas, VA) cultured at 37°C and 5% CO_2 in DMEM supplemented with 1% sodium pyruvate, 1% penicillin–streptomycin, 1.5 g l^{-1} $NaHCO_3$, and 10% fetal bovine serum (cDMEM). Cells were seeded at a density of 15,000 cells per well for NIH/3T3 cells and 20,000 cells per well for HEK293T cells in 48-well plates (300 μl total volume) and added immediately after complex immobilization. Transfection results were obtained 24 h post-transfection by measuring the extent of transgene expression, as quantified by the luciferase activity, using the Luciferase Assay System (Promega, Madison, WI). The luminometer was set for a 3 s delay with signal integration for 10 s. Luciferase activity was normalized to the amount of total protein in the sample, which was measured using a BCA assay (Pierce, Rockford, IL) following the manufacturer's instructions.

2.5. Visualization of fluorescently labeled DNA and cells

Plasmids encoding for β-galactosidase were labeled with Cy3 using a Label IT nucleic acid labeling kit (Mirus, Madison, WI) according to the manufacturer's instructions. Briefly, DNA and Label IT reagents were mixed and incubated at 37°C for 1 h. After incubation, DNA was precipitated with 70% ethanol and resuspended in 10 μl Tris–EDTA (TE) buffer.

To visualize lipoplex morphology and cells on the surface, lipoplexes formed with Cy3-labeled DNA were immobilized onto 8-well glass chamber slides (Nalge Nunc International, Rochester, NY) immediately following complex formation by incubation with the substrate for 2 h. NIH/3T3 cells were added immediately after lipoplex immobilization and allowed to incubate at 37°C and 5% CO_2 overnight. An inverted Leica LCS DM-IRE2 confocal microscope was used to image peptide–lipoplexes and live cells, which were imaged through a ×40 oil-immersion objective with a field of view of 375 × 375 μm, with *Z*-sections taken every 366.3 nm. The resulting image resolution was 2048 × 2048 pixels, and *Z*-sections were taken to image the entirety of cells within the *X*, *Y* field of view, producing a voxel size of 183 × 183 × 366 nm (*X*, *Y*, *Z*). Cy3-labeled plasmid DNA was excited by a 1 mW GreNe laser at 543 nm and fluorescence was observed at 555-600 nm. Lysosomal compartments were visualized by incubating cells with 0.5 μl Lysotracker Yellow HCK-123 for 30 min at room temperature prior to excitation with a 5 mW Ar laser at 488 nm and fluorescence was observed at 495-533 nm. Nuclear compartments were visualized by incubating cells with 0.2 μl Syto 61 nucleic acid stain for 5 min at room temperature prior to excitation by a 10 mW HeNe laser at 633 nm and fluorescence was observed at 645-725 nm. Sequential scanning was used to control for spectral overlap between fluorophores, with 2× line averaging to improve signal-to-noise ratios.

2.6. Release of lipoplexes from the surface

The amount of DNA released from the surface as a function of time was monitored using plasmids radiolabeled with [α-^{32}P]dATP. Briefly, a nick translation kit (Amersham Pharmacia Biotech, Piscataway, NJ) was used following the manufacturer's protocol with minor modifications. Complexes were formed with radiolabeled DNA as described above and immobilized onto a 96-well plate. Immobilized complexes were washed twice to remove unbound complexes, then exposed to 100 μl of DMEM supplemented with 1% sodium pyruvate, 1% penicillin–streptomycin, 1.5 g l^{-1} $NaHCO_3$ and 10% fetal bovine serum (cDMEM). Release studies were performed at 37°C and 5% CO_2. At various time points, the amount of DNA released from the surface was determined by removing 10 μl of media from the wells and immersing samples in 5 ml of scintillation cocktail (Biosafe II, Research Products International Corp., Mount Prospect, IL) for measurement with a scintillation counter. The counts were correlated to DNA concentration using a standard curve and results were reported as the percent of DNA released on a cumulative basis.

2.7. Cellular distribution of radiolabeled plasmids

The amount of cell-associated radiolabeled DNA was determined by harvesting cells from the substrate and adding samples to scintillation cocktail. Cultured cells in 48-well plates were washed once with PBS (300 μl), exposed to trypsin (300 μl) for 3 min and quenched with 600 μl of cDMEM. Cells were further dislodged from the surface using a cell scraper. Cells were then centrifuged at 500 *g* for 5 min and resuspended in PBS (500 μl) for subsequent counting. Quantities of DNA per cell were calculated by dividing the total amount of DNA associated with cells by the number of cells seeded.

Quantification of internalized radiolabeled DNA was performed as described previously with minor modifications [18]. For quantification of internalized DNA delivered by peptide–lipoplexes, cultured cells in 12-well plates were washed once with PBS (400 μl), exposed to trypsin (400 μl) for 3 min and quenched with cDMEM (1000 μl). Cells were further dislodged from the surface using a cell scraper. Harvested cells were suspended in 100 μl of CellScrub Buffer (Gene Therapy Systems Inc.) to remove cell-surface-bound lipoplexes. The cell suspension was incubated at room temperature for 30 min, then centrifuged at 2000 rpm for 3 min. The cells were then resuspended in PBS for subsequent counting. DNA internalization efficiency was calculated as internalized plasmids per cell divided by cell-associated plasmids per cell.

2.8. Subcellular quantification of peptide–lipoplexes

Confocal microscopy, described above, was used to quantify subcellular localization of DNA complexes within lysosomes and nuclei as a percentage of cytoplasmic and cellular totals, respectively. Quantification of lipoplex localization within subcellular compartments was performed using NIH ImageJ (http://rsb.info.nih.gov/ij/). Several plug-ins were used to facilitate colocalization. Adaptive3DThreshold, a part of the MBF “ImageJ for Microscopy” Collection (www.macbiophotonics.ca/imagej/), was used to identify cytoplasmic and nuclear compartments based on the differential intensity of Syto 61 staining of cytoplasmic mRNA and nuclear DNA. The Object Counter3D plugin (http://rsb.info.nih.gov/ij/plugins/track/objects.html) was used to define nuclear and cellular compartments based upon their volumes, allowing multiple cells to be identified and characterized simultaneously. ColocalizationHighlighter, also part of the MBF Collection, was used to colocalize plasmid DNA to cytoplasmic, lysosomal or nuclear compartments. Colocalized voxels were counted and compared to total cellular or cytoplasmic DNA for each condition. At least 25 cells were captured per image stack, and at least five image stacks were taken per condition.

2.9. Inhibition of endocytosis

Cells were cultured with immobilized peptide–lipoplexes as described above in the presence of endocytic inhibitors, specifically chlorpromazine to inhibit clathrin-mediated endocytosis, amiloride to inhibit macropinocytosis, and filipin to inhibit caveolae-mediated endocytosis [19,20]. Prior to seeding onto the immobilized complexes, NIH/3T3 cells were split, counted and diluted in endocytic inhibitor-containing media to a concentration of 215,000 cells ml^{-1}. Cells were incubated with 5 mM amiloride for 10 min, 1 μg ml^{-1} filipin for 30 min or 10 μg ml^{-1} chlorpromazine for 30 min at 37°C and 5% CO_2, then seeded into wells with immobilized complexes in cDMEM containing the same concentration of endocytic inhibitor. Luciferase expression levels were measured as described above. Results are reported as relative transfection compared to transfection without endocytic inhibitors.

2.10. Statistics

Statistical analysis was performed using JMP software (SAS Institute, Inc., Cary, NC). Comparative analyses were completed using one-way ANOVA with Tukey post hoc tests, at a 95% confidence level. Mean values with standard deviation are reported and all experiments were performed in triplicate.

3. Results

3.1. Peptide content and substrate-mediated lipofection efficiency

Surface delivery of lipoplexes formed at peptide/DNA ratios of 10 and 100 significantly increased reporter protein expression in NIH/3T3 mouse fibroblasts compared to lower peptide/DNA ratios with SV40 peptide (Fig. 1). The addition of cationic peptide increased protein expression by up to 4.6-fold compared to lipoplexes without peptide. This trend was also observed in NIH/3T3 cells with the scrambled peptide, sSV40, and with both peptides in HEK293T human embryonic kidney cells (data not shown). These and subsequent results in this report indicated that the enhancement in gene delivery is not sequence-specific; thus, only results with SV40 peptide are presented.

3.2. Morphology of immobilized peptide–lipoplexes with cells

Lipoplexes formed with Cy3-labeled DNA demonstrated that the particle size and distribution of peptide–lipoplexes on the surface was a function of peptide content. Peptide–lipoplex average diameters and zeta potentials in solution were previously measured, with peptide/lipoplexes formed at peptide/DNA ratios of over 100 having similar diameters to lipoplexes without peptide (~250 nm) [14]. However, after 24 h on the surface, peptide–lipoplexes formed at a peptide/DNA ratio of 100 had marked aggregation on the surface relative to peptide/DNA ratios of 10 or less and appeared less homogeneously distributed (Fig. 2). In addition, smaller aggregates of Cy3-labeled DNA are apparent in the cell body at low peptide amounts relative to higher peptide amounts. Since lipoplexes with and without peptide have similar diameters in solution, the increased aggregation of peptide containing lipoplexes after 24 h on the surface suggests weaker interaction with the surface compared to lipoplexes without peptide, which was subsequently investigated in terms of the release profile.

3.3. DNA release from the surface

Cumulative release of immobilized DNA from the surface was subsequently quantified to investigate surface stability. The amount of DNA bound to the surface after washing was not a function of peptide/DNA ratio (data not shown). Peptide–lipoplexes formed at a peptide/DNA ratio of 100 had significantly more DNA released in the media compared to other conditions ($p<0.05$) at the earliest time point (5 h). This difference was reduced and not statistically significant relative to lipoplexes without peptides at later time points (Fig. 3). Interestingly, peptide–lipoplexes formed at a peptide/DNA ratio of 100 were previously found to have negative zeta potentials, while peptide–lipoplexes formed at peptide/DNA ratios below 40 have positive zeta potentials [14]. This difference in zeta potential may explain the different morphology and release rate observed for peptide–lipoplexes formed at a peptide/DNA ratio of 100 compared to those formed at lower peptide/DNA ratios.

3.4. Cellular association and internalization of DNA

The mechanism of transfection enhancement was investigated by quantifying cellular association and the internalization efficiency of DNA. The inclusion of peptide with lipoplexes at a peptide/DNA ratio of 10 and 100 decreased cellular association by up to 2.8-and 5.9-fold, respectively, compared to lipoplexes without peptide (Fig. 4A). Despite significant differences in cell-associated DNA as a function of peptide content, the number of internalized plasmids

per cell was not significantly different among the different peptide/DNA ratios, with 2.3–3.0 $\times 10^4$ plasmids internalized (Fig. 4B). These results indicated a 4.5-fold increase in internalization efficiency, which was defined as the percentage of cell-associated DNA that is internalized, with lipoplexes formed at a peptide/DNA ratio of 100 compared to lipids alone (Fig. 4C).

3.5. Lysosomal escape

Subsequent studies were performed to quantify the relative distribution of lipoplexes within lysosomes, which is a significant barrier to efficient gene transfer. Confocal microscopy was utilized to determine the amount of lysosomal DNA in cells as a percentage of cytoplasmic DNA. Representative confocal microscopy images from which lysosomal and nuclear DNA percentages were quantified are shown in Fig. 5. DNA aggregates appeared larger for peptide–lipoplexes formed at a peptide/DNA ratio of 100 (Fig. 5D) compared to the other conditions. At a peptide/DNA ratio of 100, the percentage of lysosomal DNA was significantly lower compared to peptide/DNA ratios of 0, 1 and 10, with a 2.1-fold decrease of lysosomal DNA percentage compared to lipids alone (Fig. 6A). A decreased amount of lysosomal DNA may indicate a larger amount of DNA available in the cytoplasm for nuclear trafficking, as DNA that is unable to escape the lysosomal compartments is likely to be degraded.

3.6. Nuclear accumulation of DNA

Nuclear accumulation of DNA was also quantified by confocal microscopy as a function of peptide content. The inclusion of peptide with lipoplexes at a peptide/DNA ratio of 100 increased nuclear accumulation efficiency of DNA by 3.0-fold compared to lipoplexes without peptide, with nuclear accumulation efficiency calculated as the percentage of intracellular DNA that is nuclear associated as measured by confocal microscopy quantification (Fig. 6B). The inclusion of peptide into lipoplexes resulted in 19.5% of intracellular plasmids co-localizing with the nuclear compared to only 6.5% with lipoplexes without peptide. Thus, the addition of peptide to lipoplexes may play a role not only in the efficiency at which lipoplexes are internalized, but also in the efficiency of nuclear trafficking of the peptide–lipoplex's DNA cargo. Nuclear association of lipoplexes was not significantly different between lipoplexes containing the SV40 peptide and the scrambled peptide (data not shown).

3.7. Internalization pathway

We subsequently tested the hypothesis that increasing the peptide content may affect the route of internalization by the cell, which may dictate intracellular trafficking and nuclear accumulation. Transfection studies were performed with internalization inhibitors, specifically amiloride to inhibit macropinocytosis, filipin to inhibit caveolae-mediated endocytosis and chlorpromazine to inhibit clathrin-mediated endocytosis. Transfection results indicate that there is no difference in transfection in the presence of endocytic inhibitors compared to controls at peptide/DNA ratios of 0, 1 and 10 with the exception of chlorpromazine, which slightly decreased transfection at a peptide/DNA ratio of 1 compared to no inhibitor (Fig. 7). Interestingly, at a peptide/DNA ratio of 100, filipin and chlorpromazine inhibit luciferase expression by an order of magnitude, with amiloride inhibiting transfection to a lesser extent. These results suggest that caveolae-and clathrin-mediated endocytosis become the predominant routes to internalization of the peptide–lipoplexes by the cell at high peptide content, though uptake by macropincytosis still makes some contribution.

4. Discussion

We report herein that the addition of cationic peptides that self-assemble with DNA and lipids is a simple and robust approach to overcome limiting steps to substrate-mediated gene delivery. Lipoplexes containing either intact or scrambled NLS peptides at peptide/DNA ratios of 10

and 100 significantly increase reporter protein expression compared to peptide/DNA ratios below 10, with an increase of up to 4.6-fold for luciferase expression in NIH/3T3 cells. Visualization of lipoplexes using fluorescence microscopy indicates morphological changes of the lipoplexes on the surface with increasing peptide amount, which may be due to increased aggregation of the lipoplexes on the surface. Despite decreasing cellular association, the internalization efficiency, lysosomal escape and nuclear accumulation of DNA increase with increasing peptide amount, indicating improved intracellular trafficking with the addition of peptide. In addition, altered endocytic pathways are observed with the addition of peptide. The approach to form self-assembling peptide–lipoplexes used herein is a robust approach to the formation of modular, or multi-functional, complexes, as different peptides can easily be substituted into the lipoplex assembly to modulate lipoplex physiochemical and biological properties.

The addition of peptide at a peptide/DNA ratio of 100 resulted in increased internalization efficiency, decreased lysosomal DNA and increased cytoplasmic DNA available to traffic to the nucleus, which is consistent with the greater nuclear accumulation of plasmid. Less cell-associated DNA was observed for the peptide–lipoplexes than for lipoplexes without peptide; however, the levels of internalized DNA were similar, which indicates greater internalization efficiency for the peptide–lipoplexes at higher peptide amounts. The reduced amount of cell-associated DNA may result from the observed aggregation of peptide–lipoplexes on the surface relative to lipoplexes without peptide. Vector aggregation may result from weaker interactions between the vector and the surface, leading to vector–vector interactions. Importantly, decreasing the strength of the vector–surface interactions may also increase the internalization efficiency. The presence of peptides also increased the efficiencies of additional intracellular trafficking steps, such as lysosomal escape and nuclear trafficking. At a peptide/DNA ratio of 100, the levels of lysosomal DNA were less than with lipoplexes without peptide, suggesting a greater ability to avoid or escape the lysosome. Finally, all conditions have similar levels of internalized DNA, yet peptide–lipoplexes formed at a peptide/DNA ratio of 100 demonstrate a greater accumulation of plasmid in the nucleus, suggesting a greater efficiency of trafficking to the nucleus.

The decrease in the lysosomal DNA levels likely reflects the relative activity of multiple internalization pathways for the vector. The degradative lysosomal pathway may be avoided through caveolae-mediated endocytosis [19-21]. In this report, the addition of filipin, which inhibits caveolae-mediated endocytosis, significantly decreased transfection at a peptide/DNA ratio of 100, suggesting that lipoplexes formed at a peptide/DNA ratio of 100 are endocytosed through caveolae more so than at lower peptide amounts. This result may account for the decrease in lysosomal DNA and increase in nuclear-associated DNA observed at a peptide/DNA ratio of 100. The peptides may potentially impact clathrin-mediated endocytosis. Clathrin-coated vesicles traverse the cytoplasm and form lysosomes; however, endosomal escape prior to the progression of endosomes to lysosomes may have occurred with increasing peptide, as peptide display on a lipid surface has been shown to enhance escape from lysosomal degradation [22,23]. Thus, an increase in clathrin-mediated endocytosis may not result in increased lysosomal localization if endosomal escape is achieved.

While a peptide/DNA ratio greater than 100 was necessary to enhance lipofection by bolus delivery [14], a peptide/DNA ratio of 10 was adequate for lipofection enhancement by surface delivery. The variation in the amount of peptide needed to enhance bolus and surface delivery of lipoplexes likely results from the rate-limiting steps for each system. Cellular association of DNA has been identified as the rate-limiting step for bolus transfection with lipoplexes, while internalization is the limiting step for surface-mediated lipofection [13,24]. The immobilization of complexes places DNA directly in the cell microenvironment, thereby overcoming mass transport limitations that reduce the barrier to cellular association by bolus

delivery; however, internalization then emerged as the limiting step for lipoplexes and the addition of peptides increased the internalization efficiency.

The addition of peptides may impart polyplex properties to lipoplexes to enhance substrate-mediated lipofection, with peptides contributing to the increased polyplex-like properties. Polyplexes delivered from the surface are limited by decreased potency due to surface immobilization [13], which may result from conformational changes or altered polymer content [25]. However, lipoplexes are limited by internalization from the surface [13]. Addition of peptides to the lipoplexes results in the presentation of peptides on the lipoplex surface, which may facilitate cellular internalization [14]. The effect of the peptide, however, is dependent upon the amount of peptide incorporated. Peptide–lipoplexes formed at a ratio of 10 have different morphologies, release rates and intracellular trafficking profiles than peptide–lipoplexes formed at a ratio of 100. These differences suggest that the mechanisms of transfection enhancement at a peptide/DNA ratio of 10 may differ from those at a peptide/DNA ratio of 100. Lipoplexes formed at a peptide/DNA ratio of 10 had significantly higher internalization efficiency than lipoplexes formed at lower peptide/DNA ratios. This increase in internalization efficiency may explain the observed increase in transfection for lipoplexes formed at a peptide/DNA ratio of 10, whereas for lipoplexes formed at a peptide/DNA ratio of 100, increased transfection may be attributed to increased lysosomal escape and nuclear association.

5. Conclusion

This report describes enhancement of substrate-mediated lipofection by the incorporation of peptides through self-assembly and indicates that lipofection enhancement is obtained through increased internalization efficiency of the peptide–lipoplexes, increased cytoplasmic DNA and increased nuclear accumulation of DNA. Internalization is a limiting step for lipofection from a substrate, and peptide/DNA ratios of 10 and above are necessary to achieve increased transfection. These results suggest that incorporating peptides into a self-assembling peptide–lipoplex is a robust mechanism through which lipoplexes can be modified, and illustrates the potential of incorporating modular components into lipoplexes for enhanced gene delivery from biomaterials.

Acknowledgments

Support for this research was provided in part by the NIH (R01 EB003806-01 (A.E.B., L.D.S.) and RO1 GM066830 (L.D.S.)), the Institute for BioNanotechnology in Medicine (IBNAM) at Northwestern University, and a Ford Foundation Predoctoral Fellowship (J.C.R.). Confocal microscopy images were obtained at the Biological Imaging Facility (BIF) at Northwestern University. ESI and MALDI-TOF mass spectrometry were performed at the Analytical Services Laboratory at Northwestern University. We would like to thank William Russin for technical assistance.

References

1. Ziauddin J, Sabatini DM. Microarrays of cells expressing defined cDNAs. Nature 2001;411:107–10. [PubMed: 11333987]
2. Bielinska AU, et al. Application of membrane-based dendrimer/DNA complexes for solid phase transfection in vitro and in vivo. Biomaterials 2000;21:877–87. [PubMed: 10735464]
3. Segura T, Volk MJ, Shea LD. Substrate-mediated DNA delivery: role of the cationic polymer structure and extent of modification. J Control Release 2003;93:69–84. [PubMed: 14602423]
4. Jewell CM, Zhang J, Fredin NJ, Lynn DM. Multilayered polyelectrolyte films promote the direct and localized delivery of DNA to cells. J Control Release 2005;106:214–23. [PubMed: 15979188]
5. Jewell CM, Zhang J, Fredin NJ, Wolff MR, Hacker TA, Lynn DM. Release of plasmid DNA from intravascular stents coated with ultrathin multilayered polyelectrolyte films. Biomacromolecules 2006;7:2483–91. [PubMed: 16961308]

6. Segura T, Chung PH, Shea LD. DNA delivery from hyaluronic acid–collagen hydrogels via a substrate-mediated approach. Biomaterials 2005;26:1575–84. [PubMed: 15522759]
7. Segura T, Shea LD. Surface-tethered DNA complexes for enhanced gene delivery. Bioconjug Chem 2002;13:621–9. [PubMed: 12009954]
8. Bengali Z, Pannier AK, Segura T, Anderson BC, Jang JH, Mustoe TA, Shea LD. Gene delivery through cell culture substrate adsorbed DNA complexes. Biotechnol Bioeng 2005;90:290–302. [PubMed: 15800863]
9. Jang JH, Bengali Z, Houchin TL, Shea LD. Surface adsorption of DNA to tissue engineering scaffolds for efficient gene delivery. J Biomed Mater Res A. 2005
10. Pannier AK, Anderson BC, Shea LD. Substrate-mediated delivery from self-assembled monolayers: effect of surface ionization, hydrophilicity, and patterning. Acta Biomaterialia 2005;1:511–522. [PubMed: 16701831]
11. Shen H, Tan J, Saltzman WM. Surface-mediated gene transfer from nanocomposites of controlled texture. Nat Mater 2004;3:569–574. [PubMed: 15258575]
12. Yoshikawa T, Uchimura E, Kishi M, Funeriu DP, Miyake M, Miyake J. Transfection microarray of human mesenchymal stem cells and on-chip siRNA gene knockdown. J Control Release 2004;96:227–32. [PubMed: 15081214]
13. Bengali Z, Rea JC, Shea LD. Efficacy of immobilized polyplexes and lipoplexes for substrate-mediated gene delivery. Biotechnol Bioeng. 2008
14. Rea JC, Barron AE, Shea LD. Peptide-mediated lipofection is governed by lipoplex physical properties and the density of surface-displayed amines. J Pharm Sci. 2008
15. Tagawa T, et al. Characterisation of LMD virus-like nanoparticles self-assembled from cationic liposomes, adenovirus core peptide mu (mu) and plasmid DNA. Gene Ther 2002;9:564–576. [PubMed: 11973632]
16. Gao X, Huang L. Potentiation of cationic liposome-mediated gene delivery by polycations. Biochemistry-Us 1996;35:1027–1036.
17. Khalil IA, et al. Octaarginine-modified multifunctional envelope-type nanoparticles for gene delivery. Gene Ther 2007;14:682–689. [PubMed: 17268535]
18. Moriguchi R, Kogure K, Iwasa A, Akita H, Harashima H. Non-linear pharmacodynamics in a non-viral gene delivery system: positive non-linear relationship between dose and transfection efficiency. J Control Release 2006;110:605–609. [PubMed: 16360229]
19. Bengali Z, Rea JC, Shea LD. Gene expression and internalization following vector adsorption to immobilized proteins: dependence on protein identity and density. J Gene Med 2007;9:668–678. [PubMed: 17533618]
20. Khalil IA, Kogure K, Futaki S, Harashima H. High density of octaarginine stimulates macropinocytosis leading to efficient intracellular trafficking for gene expression. J Biol Chem 2006;281:3544–3551. [PubMed: 16326716]
21. Rejman J, Bragonzi A, Conese M. Role of clathrin-and caveolae-mediated endocytosis in gene transfer mediated by lipo-and polyplexes. Mol Ther 2005;12:468–474. [PubMed: 15963763]
22. El-Sayed A, Khalil IA, Kogure K, Futaki S, Harashima H. Octaarginine- and octalysine-modified nanoparticles have different modes of endosomal escape. J Biol Chem. 2008
23. Khalil IA, Kogure K, Futaki S, Harashima H. Octaarginine-modified liposomes: enhanced cellular uptake and controlled intracellular trafficking. Int J Pharm 2008;354:39–48. [PubMed: 18242018]
24. Varga CM, Tedford NC, Thomas M, Klibanov AM, Griffith LG, Lauffenburger DA. Quantitative comparison of polyethylenimine formulations and adenoviral vectors in terms of intracellular gene delivery processes. Gene Ther 2005;12:1023–1032. [PubMed: 15815703]
25. Pannier AK, Wieland JA, Shea LD. Surface polyethylene glycol enhances substrate-mediated gene delivery by nonspecifically immobilized complexes. Acta Biomaterialia 2008;4:26–39. [PubMed: 17920004]

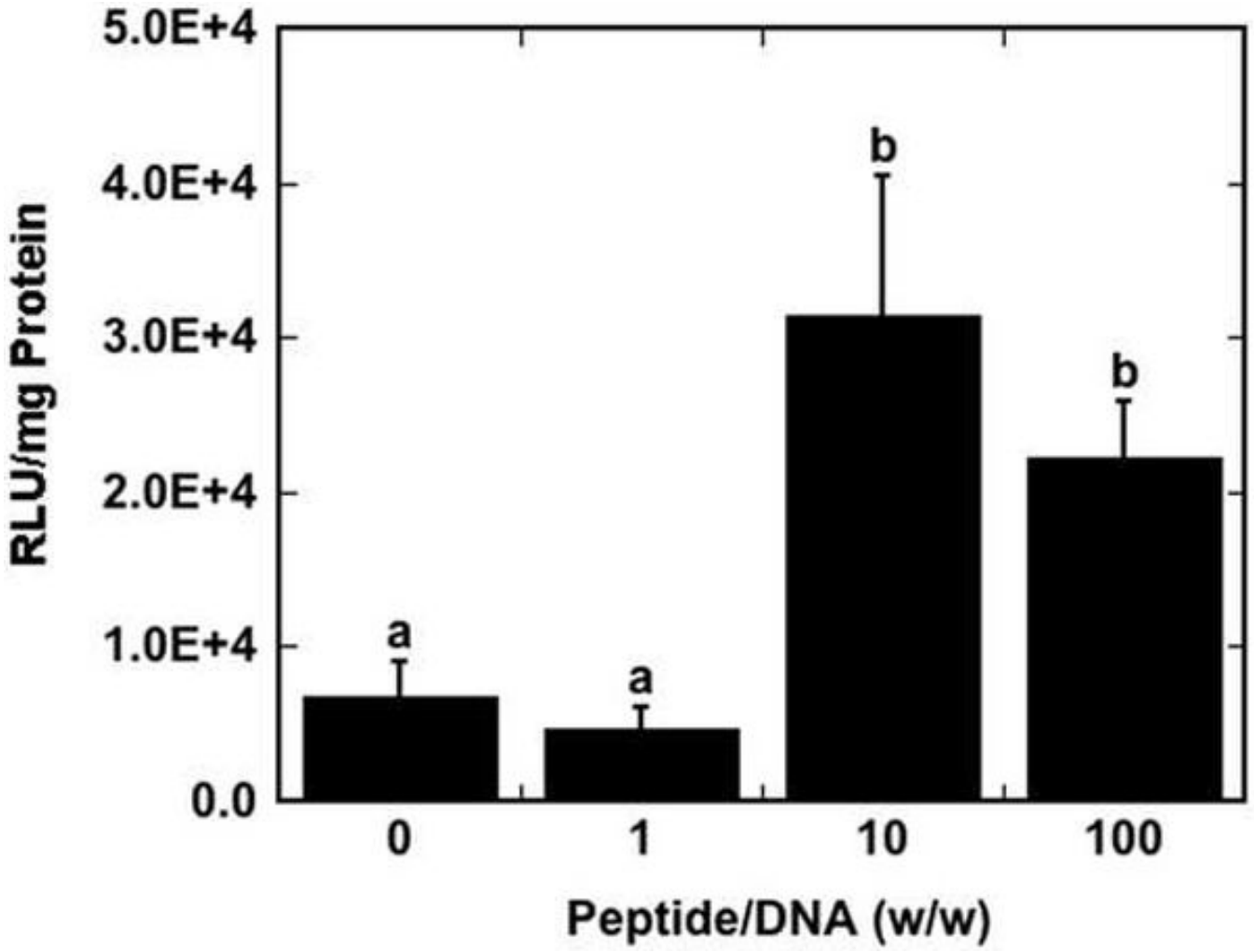

Fig. 1.

Transfection of NIH/3T3 cells as a function of peptide/DNA ratio. Luciferase expression levels are reported as relative light units (RLU) normalized by total protein in the sample well. Data are presented as the mean of triplicate measurements ± standard deviation. A statistical significance with $p<0.05$ is denoted for values with different letters.

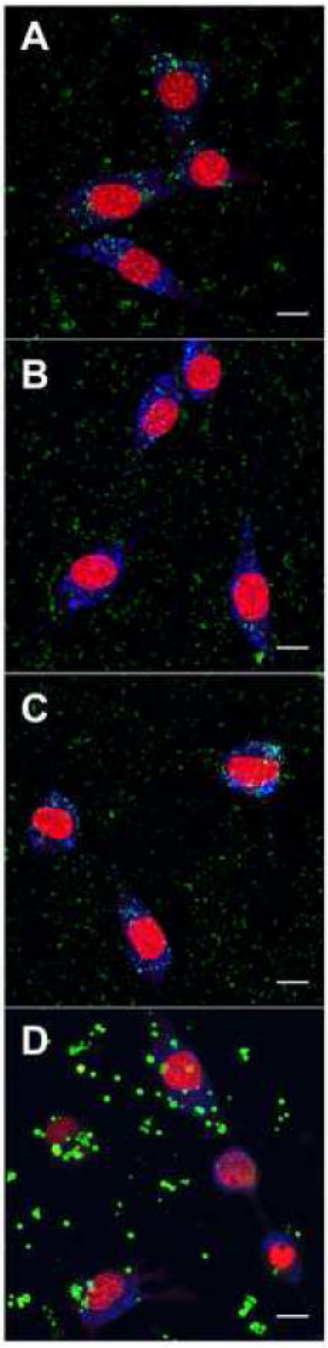

Fig. 2.

Visualization of cells and immobilized DNA. Cy3-labeled DNA complexes were immobilized onto tissue-culture polystyrene and visualized with NIH/3T3 cells using confocal microscopy. Z-projections of maximum intensity are shown. Green indicates Cy3-labeled DNA, blue indicates lysosomes and red indicates nuclei. Scale bars represent 40 μm. Peptide/DNA ratios (w/w) are as follows: 0 (A), 1 (B), 10 (C) and 100 (D).

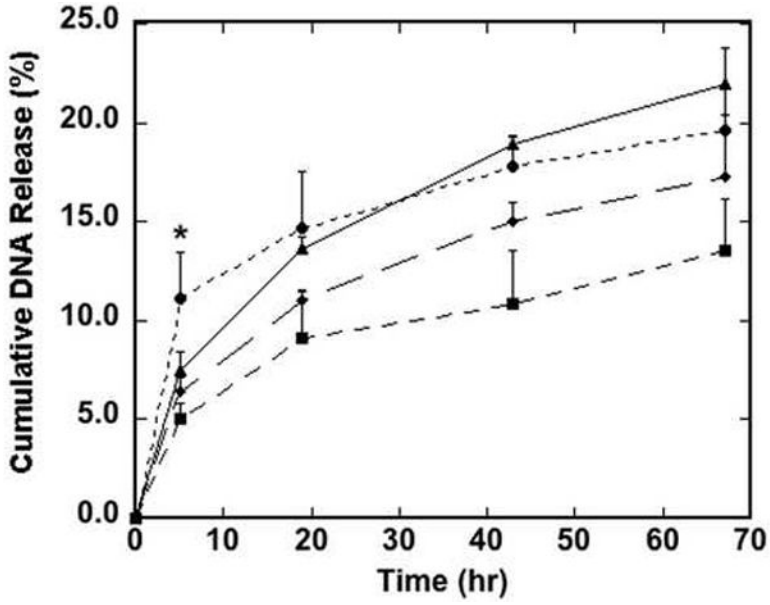

Fig. 3.

Cumulative release of DNA from the surface as a function of time. Peptide–lipoplexes containing radiolabeled DNA at peptide/DNA ratios of 0 (▲), 1 (◆), 10 (■) and 100 (●) were immobilized to tissue-culture polystyrene and exposed to serum-containing media. Cumulative release of DNA was measured as various time points by extracting samples from the media and measuring DNA content using a scintillation counter. Data are presented as the mean of triplicate measurements ± standard deviation (*p<0.05).

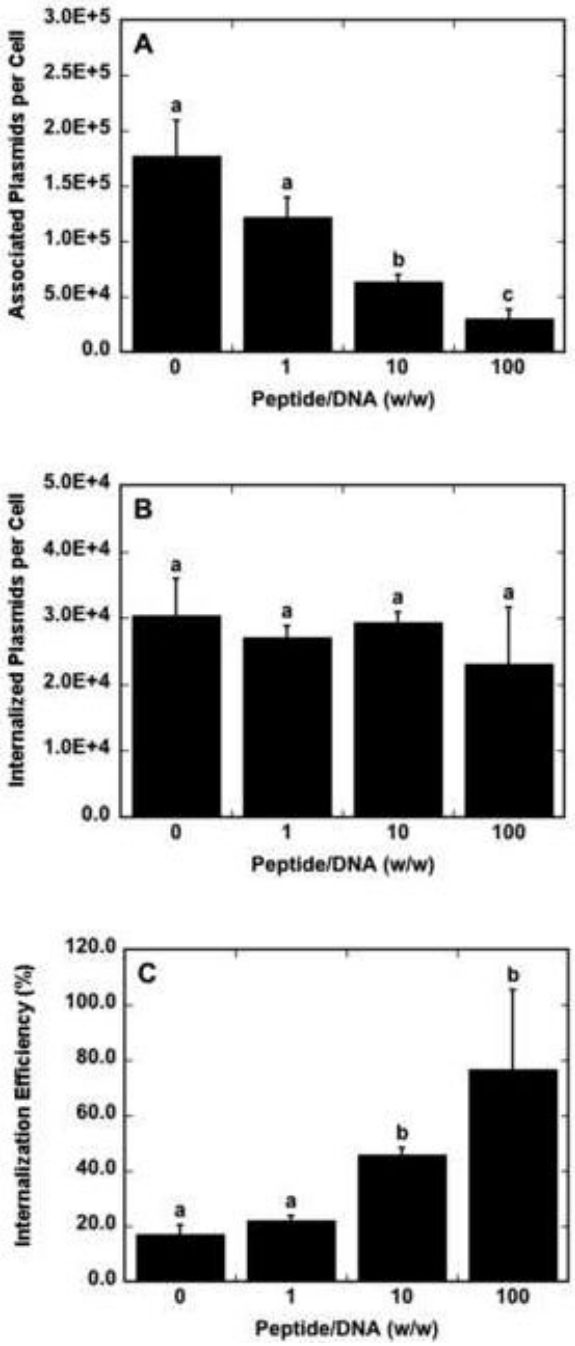

Fig. 4.

Cell association and internalization of DNA as a function of peptide content. Peptide–lipoplexes containing radiolabeled DNA were immobilized to tissue-culture polystyrene prior to the addition of NIH/3T3 cells. Cell-associated plasmids (A) and internalized plasmid copies (B) are reported per cell. Internalization efficiency (C) was calculated as the percentage of cell-associated plasmids that are internalized per cell. Data are presented as the mean of triplicate measurements ± standard deviation. A statistical significance with $p<0.05$ is denoted for values with different letters.

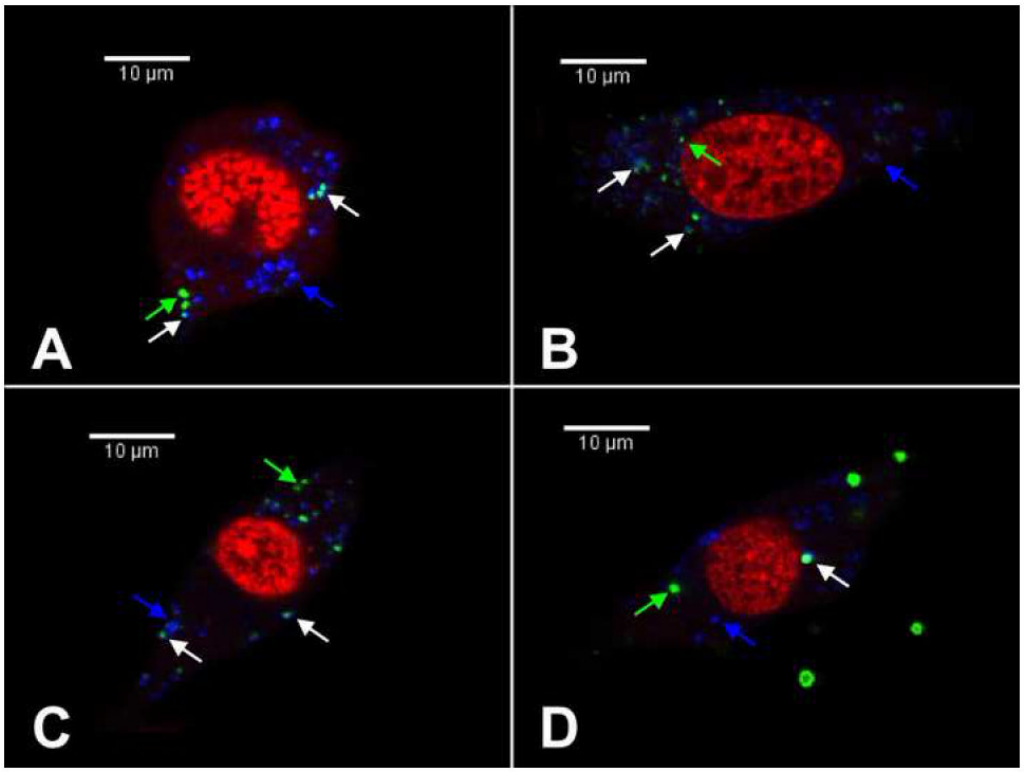

Fig. 5.

Confocal microscopy images depicting colocalization of plasmid DNA and subcellular compartments. NIH/3T3 cells were incubated with immobilized lipoplexes for 24 h prior to imaging. Cells with peptide–lipoplexes formed at peptide/DNA ratios of 0 (A), 1 (B), 10 (C) and 100 (D) are shown. Red indicates nucleic acid staining, green indicates Cy3-labeled plasmid DNA and blue indicates lysosomal staining. Green arrows indicate non-lysosomal DNA, white arrows indicate DNA colocalized with lysosomes and blue arrows indicate lysosomes without Cy3-labeled DNA. A single *Z*-section representative of the sample is shown for each condition.

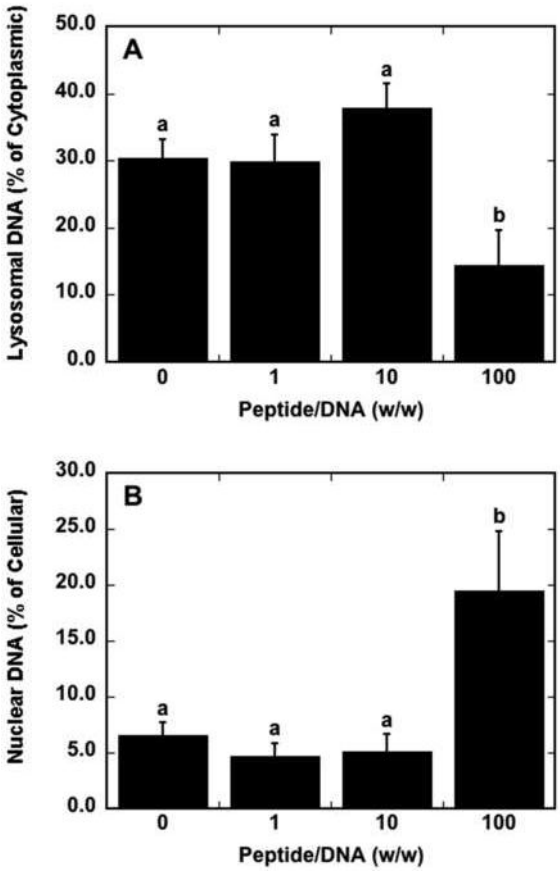

Fig. 6.

Lysosomal escape and nuclear accumulation efficiencies of plasmids as a function of peptide content. The percentage of cytoplasmic DNA that is co-localized with lysosomes (A) and the percentage of intracellular DNA that is co-localized with nuclei (B) as calculated from confocal microscopy images are shown. Data are presented as the mean of triplicate images containing at least 25 cells ± standard deviation. A statistical significance with $p<0.05$ is denoted for values with different letters.

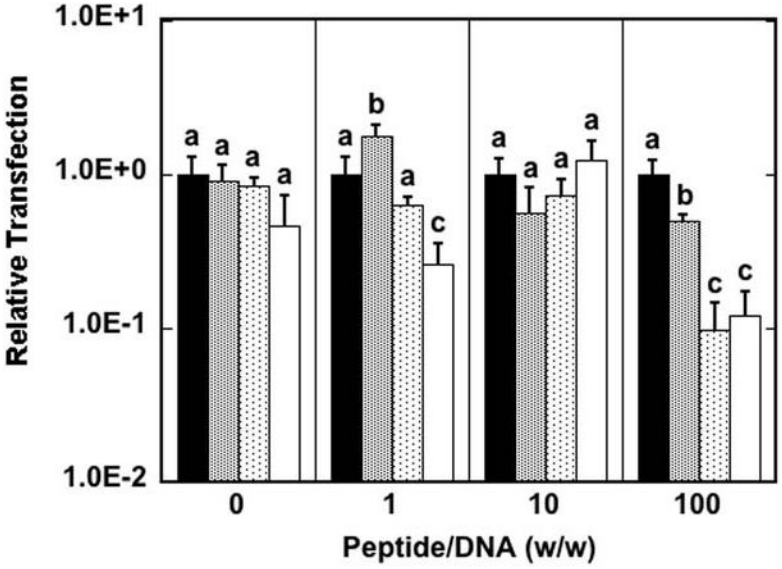

Fig. 7.

Internalization pathways of DNA as a function of peptide content. Transfection was performed at various peptide/DNA ratios without endocytic inhibitors (black bars) or in the presence of amiloride (gray bars), filipin (dotted bars) or chlorpromazine (white bars). Transfection with inhibitor is reported relative to transfection without inhibitor. Data are presented as the mean of triplicate measurements ± standard deviation. A statistical significance with $p<0.05$ is denoted for values with different letters, with comparisons made only within the same peptide/DNA ratios.